Front. Mater. Sci. 2016, 10(3): 290–299
DOI 10.1007/s11706-016-0349-5

RESEARCH ARTICLE

Natural sunlight irradiated flower-like CuS synthesized from DMF solvothermal treatment

Wei ZHAO (✉), Zihao WANG, Lei ZHOU, Nianqi LIU, and Hongxing WANG

School of Materials Science and Engineering, Tianjin Chengjian University, Tianjin 300384, China

ABSTRACT: Three-dimensional CuS hierarchical crystals with high catalytic activity had been successfully fabricated using a facile solvothermal process. The CuS microparticles showed different flower-like morphology and good dispersion by optimizing reaction conditions. It was found that using N,N-dimethylformamide (DMF) as the solvent reagent in the proper temperature conditions was favorable for the growth of hierarchically structured CuS. The hexagonal flower-like CuS synthesized at 170°C for 60 min displayed broad-spectrum photocatalytic properties under ultraviolet (UV) and visible irradiation. The as-prepared CuS crystals exhibited good performance to decolorize methylene blue (MB) solution under visible light irradiation. The total organic carbon (TOC) removal of rhodamine B (RhB) solution was nearly 60% after 5 h of the natural sunlight irradiation, and the property was stable after testing over four recycles, demonstrating a potential application in waster water treatment.

KEYWORDS: photocatalysis; CuS; hierarchical structure; natural sunlight irradiation

Contents

1 Introduction
2 Experimental
  2.1 Materials
  2.2 Synthesis of CuS photocatalyst
  2.3 Characterization
  2.4 Photocatalytic experiments
3 Results and discussion
  3.1 Characterization of CuS
  3.2 Plausible formation of hierarchical microflowers of CuS
  3.3 Visible-light photocatalytic activity of CuS samples
4 Conclusions
Acknowledgements
References

Received May 5, 2016; accepted June 12, 2016

E-mail: zhaowei2004@tsinghua.org.cn

1 Introduction

As a by-product of industrialization, large amounts of waster water flow into our river systems, carrying organic pollutants that pose a serious threat to human health. This has become a major topic of study for researchers. A number of methods such as adsorption of the organic pollutants, precipitation or reduction of the metal ions have been devised to treat these pollutants using nitro-based organic compounds, coloring agents and waster water laden with heavy metals. Among these reported methods, photocatalytic degradation with nontoxicity, chemical

stability has emerged as a cost-effective option for removing organic pollutants [1–4]. Photocatalysts that effectively utilize visible light, such as sulphides [5–8], nitrides [9–11], oxides and Bi-based compounds [12–13], have also been widely studied in recent years. Among them, materials with one-dimensional morphology [14], hollow shape [15], hierarchical structures [16] are easy to have excellent performance attributing to the large surface area and good transportation for the electrons or holes irradiated by the light.

CuS is an important semiconducting nanomaterial with a direct band gap. It has various potential applications in photoelectric devices, lithium batteries, chemical sensors, thermoelectric cooling materials, high-capacity cathode materials, solar cells, optical filters, superionic materials, photocatalysts and so forth [17–21]. So far, various morphologies of CuS including nanoflakes, flower-like nano-micro structures, cave-like structures and hollow spheres have been reported [22–24]. Hierarchical structures significantly enhance the performance of materials due to their nano-sized building blocks and micro- or submicro-sized assemblies [25]. The hierarchical structured CuS could show mono-dispersible nature and a large specific surface area to improve photocatalytic performance. On the one hand, the constructed assemblies of the micrometer-sized particles will allow the photocatalyst to be easily recovered from the working suspension after use, and the nanometer-sized building units, on the other side, provide a greater available surface area for dye loading. At present, some research have reported the good photocatalytic activities of the hierarchical structured CuS through solvothermal methods, most of them could decolorize methylene blue (MB) and rhodamine B (RhB) organic contaminant within 1 h [26–29]. However, some of them have a time-consuming synthesis process, many researchers choose ethylene glycol (EG) and water as the solvent, and the reactant time is up to 24 h [30–31]. Additionally, rare work has been done to explore the real degradation behavior of the CuS particles, for instance, the total organic carbon (TOC) test. And the selection of the light source is mainly based on visible light or ultraviolet light. There are few reports about the photo degradation behavior of CuS under the natural sunlight exposure. Herein, we report a CuS hierarchical structures that can be tailored by a simple solvothermal method using N,N-dimethylformamide (DMF) as solvent, which has shorten the synthetic time. And the excellent photocatalytic degradation properties of CuS irradiated by natural sunlight could be achieved and promote the application in waster water treatment.

2 Experimental

2.1 Materials

Copper(II) chloride ($CuCl_2 \cdot 2H_2O$, 99%), thiourea (CH_4N_2S, 98%), DMF ($>99.5\%$), H_2O_2 (AR), ethyl alcohol (EtOH, AR), MB (AR) and RhB (AR) were purchased from Tianjin Jizhun Agent Company and used as received. All the chemicals were of analytical grade and used without further purification. Deionized water and EtOH were used as the solvent to wash the as-prepared CuS powders.

2.2 Synthesis of CuS photocatalyst

Typically, 4 mmol of $CuCl_2 \cdot 2H_2O$ was dissolved in 30 mL of DMF solution, forming a slight green solution under constant stirring for 10 min, and a thiourea (Tu)–DMF transparent solution prepared by dissolving 10 mmol of thiourea into 30 mL of DMF solution. These two solutions were mixed under magnetic stirring for 45 min. A red suspension was formed and transferred into a 100 mL Teflon-lined autoclave and maintained at 160°C–180°C for 45–90 min. The resulting solution was allowed to cool to room temperature naturally. The black precipitate was filtered off, washed in deionized water and absolute ethanol several times and dried at 60°C for 4 h to obtain the final product. In a comparison synthesis procedure, CuS hierarchical structures were also prepared by adding amount of polyvinylpyrrolidone (PVP) surfactant to the mixed red suspension while preserving all other above-mentioned reaction parameters.

2.3 Characterization

Samples were analyzed by X-ray diffraction (XRD, Ragaku 2500) with Cu Kα radiation at a scan rate of 6 min^{-1}, in the 2θ range of 10°–80°. The morphology of the samples was examined by field emission scanning electron microscopy (FESEM, JEOL 6700F, accelerating voltage = 10 kV) and high-resolution transmission electron microscopy (HRTEM, JEOL JEM-2100F, accelerating voltage = 100 kV). A Shimadzu UV-3100 spectrophotometer was used to record the optical absorption spectra of the samples using $BaSO_4$ as the reference material.

2.4 Photocatalytic experiments

To evaluate catalytic activity at ambient temperature, a series of comparative experiments were carried out under (separately) an Xe lamp, visible light lamp and natural sunlight for decolorization with the assistance of hydrogen peroxide (H_2O_2, 30% (w/w)).

The application of CuS for the degradation of organic dye MB was investigated under visible-light irradiation in an open cylindrical reactor at room temperature. Typically, a 50 mg amount of photocatalyst powder was suspended in 100 mL MB solution (10 mg/L) and 2 mL of H_2O_2. The aqueous suspension was magnetically stirred in the dark for 30 min to ensure adsorption equilibrium. Visible light radiation exposures were performed using the Xe lamp (300 W, PLS-SXE300) coupled with a UV-cut-off filter (400 nm). 3 mL of the solution was withdrawn at different irradiation times (10–60 min) and centrifuged to remove CuS particles. The above liquid was then monitored using a UV-1700 spectrometer at 662 nm.

The photocatalytic performance of CuS on another organic dye, RhB, was also tested under natural sunlight in the presence of H_2O_2. A volume of 50 mL of RhB solution was mixed with 25 mg (photocatalyst load of 1.0 $g \cdot L^{-1}$) of the CuS powder. Afterwards, 1 mL of H_2O_2 was added into the solution to set in the dark condition for 30 min, followed by further magnetic stirring under natural sunlight. All these experiments were performed at the same time to ensure uniform irradiation density among the photocatalytic reactions.

TOC of RhB dye under different irradiation times was measured using a Shimadzu TOC analysis system (TOC-V_{CPH}, Japan).

3 Results and discussion

3.1 Characterization of CuS

Figure 1 shows the XRD pattern of CuS powders at 170°C for 60 min in the absence of surfactant. The diffraction peaks are indexed with standard hexagonal CuS phase. The cell parameters are a = 3.792 Å and c = 16.344 Å. From the XRD patterns, it can be seen that the resultant product is of pure phase. The broader diffraction peaks show the smaller size of crystal formation. The XRD pattern clearly shows peaks at (101), (102), (103), (006), (110), (108) and (116) in accordance with the JCPDS file (06-0464), indicating that CuS exists as a covellite phase.

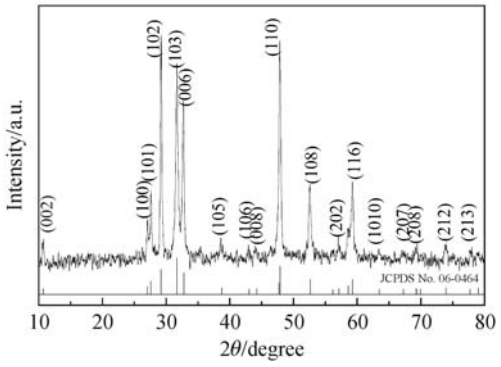

Fig. 1 XRD pattern of CuS synthesized from solvothermal process at 170°C for 1 h.

To investigate the effect of the reaction temperature on the formation of CuS hierarchical structures, a series of comparative experiments are carried out using similar processes. Typical scanning electron microscopy (SEM) images of the CuS crystals are shown in Fig. 2. As it shows, when the reaction temperature is at 160°C for 1 h, the product is composed of ball flower structures with diameters of 4–6 μm (Fig. 2(a)). This sphere-like structure consists of hundreds of self-assembled, well-arranged and oriented nanoflakes (see the inset of Fig. 2(a)). The thickness of the nanoflakes is less than 50 nm. At a higher reaction temperature of 165°C (Fig. 2(b)), the nanoflakes assemble more openly and grow much larger, and the CuS ballflower structures become hexagonal flower structures. No obvious changes are observed in the morphology of CuS synthesized at the higher reaction temperature of 170°C (Fig. 2(c)). However, the morphology of the hierarchical flower-like structured CuS becomes homogeneous and the size of the flowers is 6–10 μm. When the reaction temperature is increased to 180°C, the flower-like shapes grow less evenly and more broken nanoflakes are observed (Fig. 2(d)).

Time-dependent experiments are carried out to investigate the evolution process of the CuS hierarchical structures. During the process, samples are collected at different time intervals from the reaction mixture. As shown in Fig. 3(a), the CuS is self-assembled into hierarchical flower-like structures consisting of close-packed nanoflakes. At the initial stage of 45 min, the flowers are hexagonal in shape with sizes of about 6–10 μm, and only a small amount of the black product is obtained (see Fig. 3(d)). When reaction time increases to 50 min, the petals gently bloom, making the flower-like shape more obvious. Most of these nanoflakes align with clearly oriented layers pointing to a shared centre, and some of the

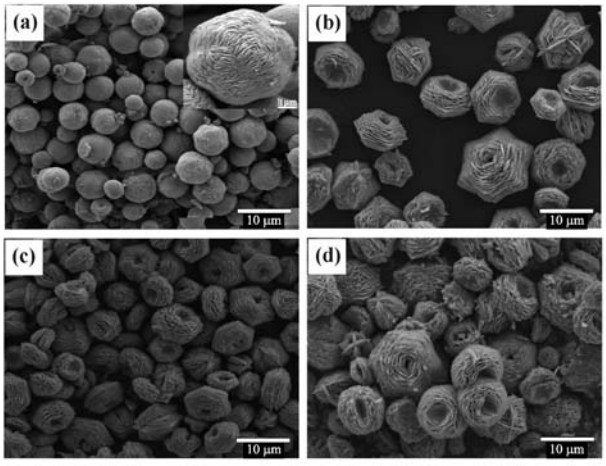

Fig. 2 SEM images of as-prepared CuS hydrothermal treated for 1 h at different temperatures: **(a)** 160°C; **(b)** 165°C; **(c)** 170°C; **(d)** 180°C.

nanosheets cross-assemble to form another flower-like shape (Fig. 3(b)). At the same time, the amount of black product increases (Fig. 3(d)). With an increase of the solvothermal time to 60 min, the sizes of the flowers are more homogeneous, as shown in Fig. 2(c), and the taxol yield peak. Finally, when the reaction is prolonged to 90 min, the cores of the spheres diminish; some flowers form nest-like structures, while others grow abnormally as demonstrated in Fig. 3(c).

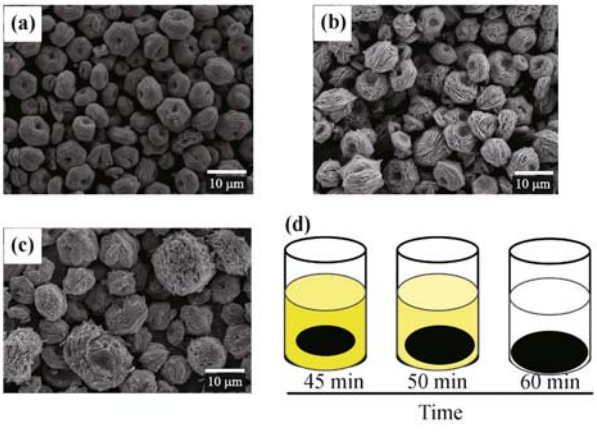

Fig. 3 SEM images of as-prepared CuS synthesized at 170°C for different time periods: **(a)** 45 min; **(b)** 50 min; **(c)** 90 min. **(d)** Schematic illustration of the CuS yield amount at various solvothermal times.

We find that morphology distribution of the CuS particle could be controlled from tailoring the thermal temperature and heating rate. At a heating rate of 3°C/min from room temperature to 140°C, and 5°C/min from 140°C to 170°C, most of the CuS particles assemble completely and exhibit a flower-like shape (see Fig. 4(a)), while changing the heating rate to 5°C/min from room temperature to 140°C, and 3°C/min from 140°C to 170°C, the number of incomplete shapes in the initial stage increases (Fig. 4(b)). CuS primary particles or CuS nuclei could not be produced until copper–thiourea complexes are solvothermally treated at 140°C. By increasing the temperature, a large number of CuS primary particles form, followed by aggregation/assembly of primary particles. Mild hydrothermal conditions at low temperatures cause more CuS nucleation, while a higher temperature and faster heating facilitate the homogeneous assembly of CuS nanostructures in a controllable manner with well-defined morphology. The EDS analysis in Fig. 4(c) indicates that the formed CuS is composed solely of Cu and S elements. The atomic percentages of Cu and S are 51.54% and 48.46% respectively, which is coincident with the stoichiometric ratio of CuS. Figure 4(d) displays a HRTEM image of the as-prepared CuS. The inset image shows the hexagonal shape of the hierarchical structure with a thin edge, being in agreement with SEM results. From the HRTEM image, the regular spacing of the clear lattice planes is calculated to be 0.311 and 0.19 nm, which is in good agreement with the interlayer spacing of the (102) and (110) crystallographic plane of hexagonal CuS. Furthermore the well-defined spots in the selected area electron diffraction pattern

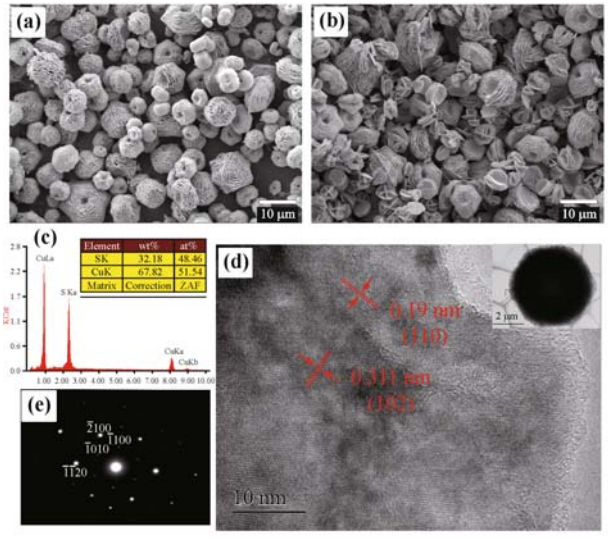

Fig. 4 SEM images of as-prepared CuS synthesized at 170°C using different heating rates: **(a)** 3°C/min from room temperature to 140°C, 5°C/min from 140°C to 170°C; **(b)** 5°C/min from room temperature to 140°C, 3°C/min from 140°C to 170°C. **(c)** EDS elemental analysis. **(d)** HRTEM image. **(e)** SAED image of the as-prepared CuS.

(Fig. 4(e)) illustrate the perfect growth of single crystals of CuS. Thus, these observations confirm that CuS microflowers have the same crystallographic orientation along the nanosheet axis as a perfect single crystal.

Figure 5 shows CuS microspheres synthesized through the DMF solvothermal process in the presence of surfactant of PVP. With the proper amount of PVP, all of the microspheres are well defined, consistent and separately displaced (Fig. 5(a)); if the amount is insufficient, there will be some small particles (Fig. 5(b)). As shown in the corresponding magnified images in Fig. 5(c) and the inset of Fig. 5(d), it can also be ascertained that the microspheres are composed of extremely thin nanosheets, hollow in nature with the nanosheets being well interconnected. From the HRTEM image, the regular spacing of the clear lattice planes is calculated to be 0.311 nm, which corresponds to the (102) lattice plane.

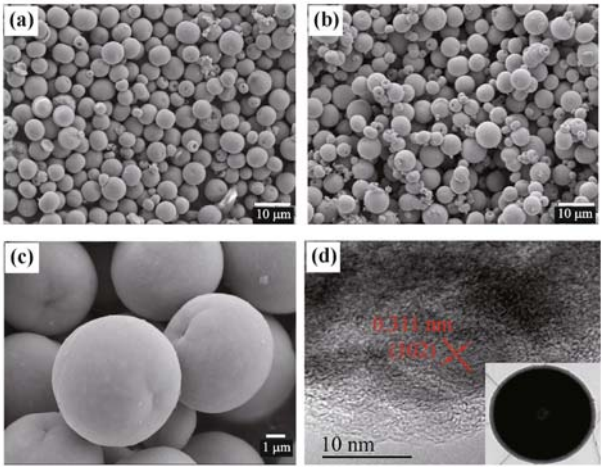

Fig. 5 SEM images of CuS samples synthesized at 170°C/1 h with different PVP content: **(a)** 1 g PVP; **(b)** 0.5 g PVP. **(c)** Magnification image of CuS with 1 g PVP surfactant. **(d)** HRTEM image of the as-prepared CuS with 1 g PVP surfactant.

3.2 Plausible formation of hierarchical microflowers of CuS

To explore the formation mechanism of the flower-shaped microspheres, time-dependent experiments were carried out. The SEM images seen in Fig. 3 show the growth process of the CuS. We also notice that some CuS microflowers have different shapes from the optimum of the reaction parameters. On the basis of the above experimental observations, we have proposed a plausible mechanism (Fig. 6) for the morphological evolution process. In the current case, the DMF solvents make the Cu^{2+} and S^{2-} dissolve and react quickly in the solution, and the initial crystal nuclei begin freely forming into the initial platelets. DMF is an important reducing agent and solvent, which shows good dissolve ability to the Cu^{2+} and S^{2-}, and improves the formation of S^{2-} ions during the reduction of S atoms. The strong affinity of Cu^{2+} and S^{2-} and the insolubility of CuS drive the reaction in the forward direction. The freshly formed nuclei with high surface energy and unstable thermodynamic activity tend to gather together quickly to minimize the interfacial energy. As the reaction proceeds, the precursor aggregations are able to grow along the oriented direction to form flakes and thus complete well-structured flower-like hexagonal superstructures. In the following secondary growth stage, a nest-like structure will appear if the reaction time is long enough. In our experiment, the whole process involves a slow nucleation of amorphous primary particles followed by a fast aggregation and crystallization of primary particles. When we lower the solvothermal temperature, the initial nuclei grow into nanoflakes and continued to grow by combining with the remaining primary particles, finally forming the ball flower structure. When we provide enough time in the initial reaction stage and proper heat energy in the secondary growth stage, the petal-like structures are able to form various complete, beautiful flower shapes.

3.3 Visible-light photocatalytic activity of CuS samples

Figure 7(A) shows the curves of the concentration of residual MB with irradiation time, both in the presence and in the absence of H_2O_2. Without catalyst CuS or in the absence of H_2O_2 (samples b and c), only a slow decrease in the concentration of MB is detected under visible-light irradiation (visible light lamp, 40 W). The adsorption activity of the CuS in the dark is also performed; only a small decrease in the concentration of MB is detected with the hexagonal CuS (sample d). The ball flower-like CuS, synthesized by solvothermal reaction with PVP surfactant, however, shows good absorbability, the adsorption on the MB reaching 70% (sample e). This could be due to the enhanced surface area of CuS with a ball flower-like shape. Figures 7(C) and 7(D) show the N_2 adsorption/desorption isotherm and the pore-size distribution (inset) of hexagonal and ball flower-like CuS, respectively. The isotherms are identified as type IV, which is characteristic of mesoporous materials. The Brunauer–Emmett–Teller (BET) specific surface area of the sample is calculated as 6.032 and 90.971 m^2/g, respectively. This high BET surface supported the

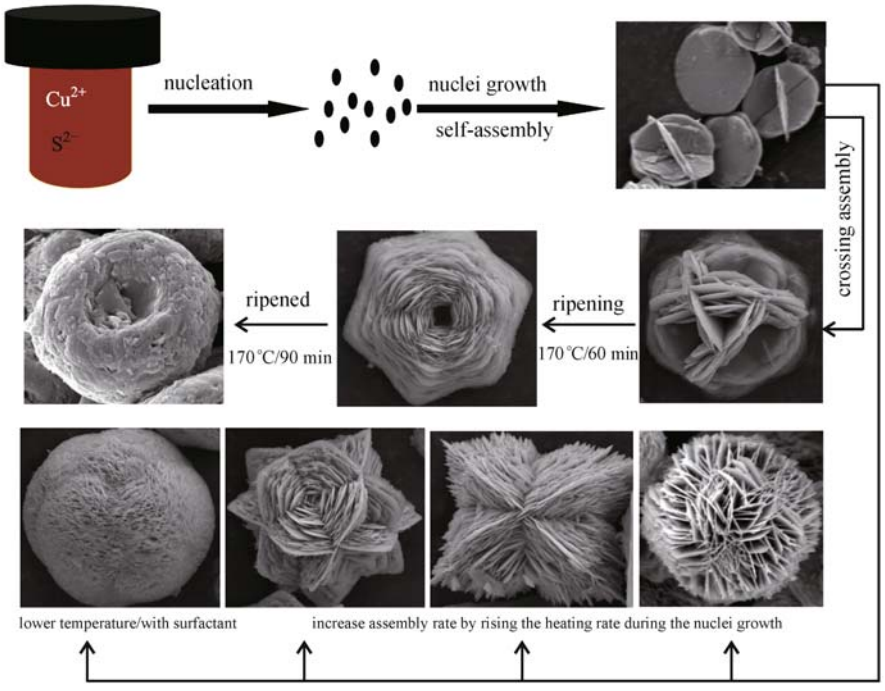

Fig. 6 Schematic illustration of the formation mechanism of the CuS hierarchical structures.

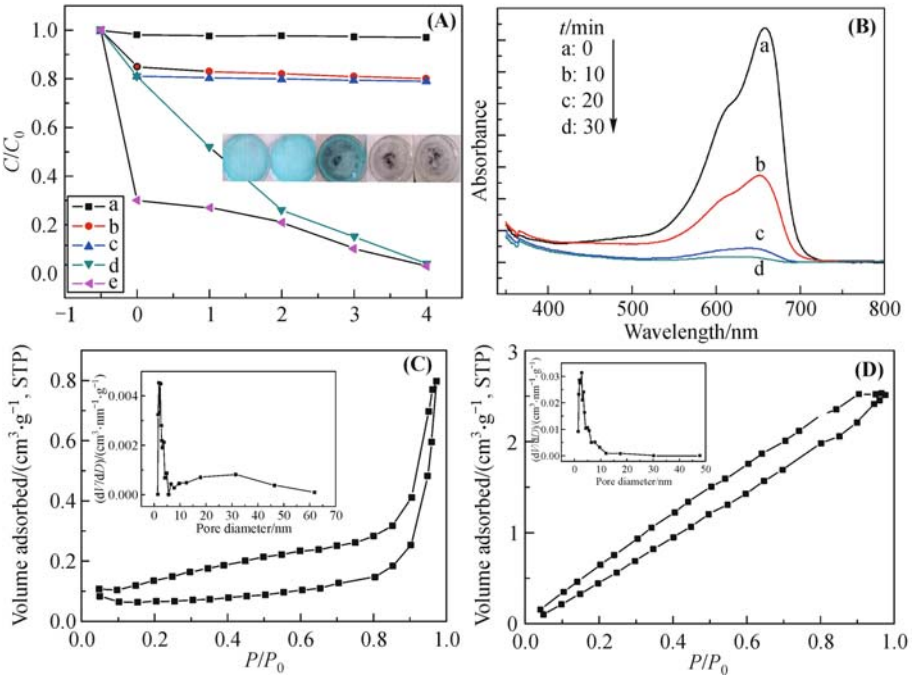

Fig. 7 **(A)** The degradation curves of MB over CuS photocatalysts: blank MB solution (a); MB solution with only H_2O_2 (b); MB solution with only hexagonal CuS (c); CuS with hexagonal flower shape + H_2O_2 (d); CuS with ball flower shape + H_2O_2 (e). **(B)** Photodegradation of CuS over MB under visible-light irradiation. **(C)** N_2 adsorption and desorption isotherms at 77 K and pore distribution of hexagonal CuS. **(D)** Ball flower-like CuS.

good adsorption on the pollutant corresponding to samples d and e in Fig. 7(A). With the help of CuS catalysts with hierarchical microarchitecture (both hexagonal CuS and ball flower-like CuS), the MB solution is decolorized

completely in 4 h. The above results show that only the simultaneous addition of catalysts and H_2O_2 could lead to an obvious degradation of MB; in the presence of peroxide, the excited electrons produced by CuS-harvested visible light could easy to be captured by oxygen in the water, which will hamper the reunion of the electrons and the holes. The remained h^+ ions are induced to react with OH^- ions accordingly in the MB solution to produce reactive oxygen species such as hydroxyl radicals that could react with organic dyes and degrade them [32–33]. The inset picture shows the color difference under the corresponding conditions.

Figure 7(B) clearly indicates that dyes of MB undergo photodegradation with CuS under visible-light irradiation (Xe lamp, 300 W), it can be seen that CuS with a hexagonal flower-like shape, synthesized at 170°C for 60 min, exhibited drastic degradation of MB immediately.

Additionally, the experimental results for RhB degradation under natural sunlight irradiation under the temperature of 26°C–28°C are investigated. As indicated clearly by the black line in Fig. 8(a), the RhB dye can be decolorized within 2 h in the presence of CuS hexagonal microflowers. Their photoreactivity over the RhB under sunlight is highly consistent with the above results for the MB degradation under visible-light irradiation. The blue line in Fig. 8(a) reveals the total carbon content, for the purpose of evaluating the mineralization ability of catalysts in the photocatalysis process. The TOC removal rate of RhB dye in the photocatalytic process (blue line) is much slower than the photodegradation of RhB dye (black line). The decolorization of RhB dye reaches 100% after 1 h of sunlight irradiation. However, a degree of mineralization of only 20% is achieved. After 5 h of irradiation, about 60% of organic carbon is removed from the solution, suggesting that the RhB is finally mineralizing under the sunlight. The inset picture shows that after 2 h of sunlight exposure, large numbers of bubbles are still being produced, indicating continuous light-degradation reactions. To illustrate the stability of CuS microsized flowers, the cycling catalytic performance of the photocatalyst is performed four times under the same conditions after centrifugal separations. As shown in Fig. 8(b), the level of photocatalytic activity of the as-prepared CuS remains high, even after being used four times for dye degradation, which indicates sufficient stability for use in environmental purification. Moreover, the recovery rate of the CuS powder reaches more than 95%, attributable to its large particle size. Figure 8(c) shows the real evaluation process for the RhB dye solution under 30–60 min irradiation in the presence of CuS powder and H_2O_2. As the time period increases, the color of the dye

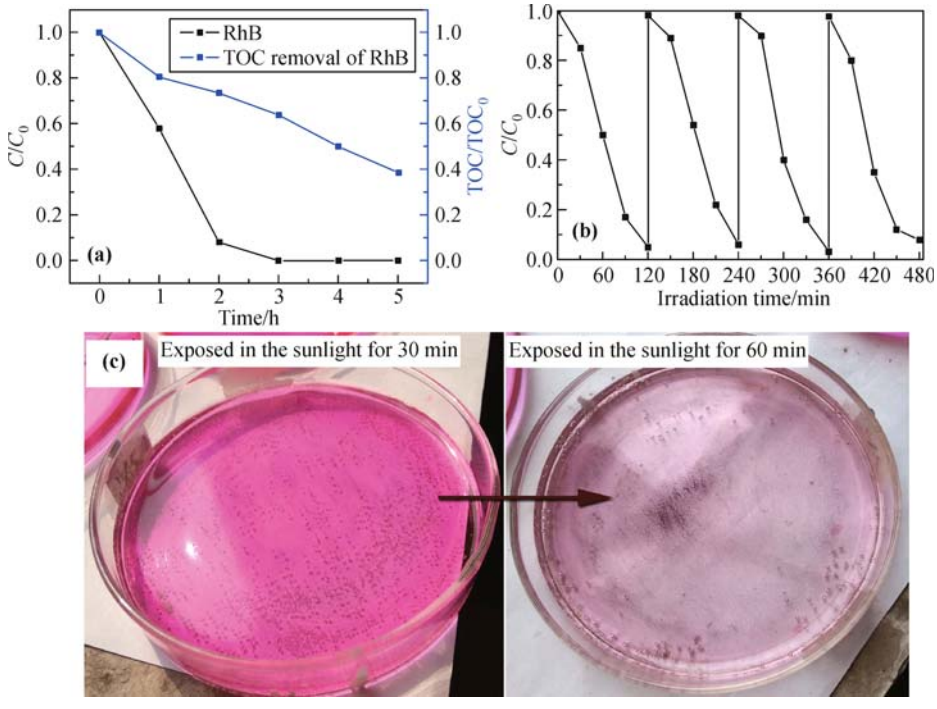

Fig. 8 **(a)** The photodegradation (black line) and TOC removal (blue line) curves of RhB dye over CuS sample under natural sunlight irradiation. **(b)** Cycling runs for the photocatalytic RhB degradation in the presence of CuS and H_2O_2. **(c)** Color changes in RhB dye over CuS sample under natural sunlight irradiation.

quickly faded and bubbles begin to form. The results demonstrate the flower-like CuS photocatalyst's strong performance in catalyzing degradation of organics and show significantly superior performances to other reported CuS samples and the commercial P25 photocatalyst, which could only degrade MB under UV irradiation.

The UV-vis diffuse-reflectance spectra of CuS are illustrated in Fig. 9(a). CuS synthesized at 170°C for 60 min present absorption in the visible light range around 600–680 nm; they exhibit a remarkable absorption in the 230–320 nm range, which could be responsible for the visible light catalytic activity and the good sunlight response. Compared with the results from the increased heating times (170°C for 75 min, 170°C for 90 min), a shorter solvothermal time results in the most efficient visible light absorption. When we increase the solvothermal time from 60 to 90 min, the morphology of CuS changes from a hexagonal flower shape to a nest-like shape, and thereby the content of sunlight harvest decreases with the absorption peak decreases accordingly. The corresponding band gaps of the samples are shown in Fig. 9(b). The approximate band gap values are estimated

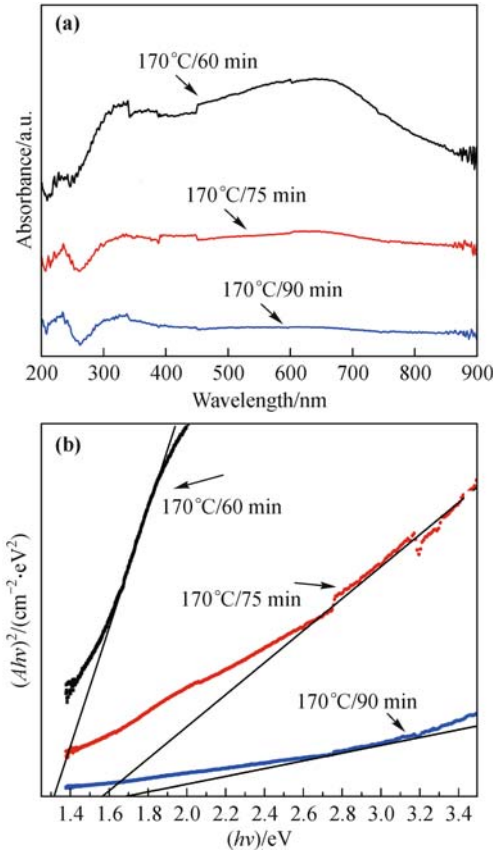

Fig. 9 **(a)** UV-visible diffuse reflectance spectra of the samples. **(b)** Tauc plots of the corresponding CuS samples.

at ~1.32, ~1.57 and ~1.7 eV, demonstrating that CuS is suitable for visible light absorption.

Overall, the enhancement in the photocatalytic property of the as-prepared CuS microflowers is most probably due to their high specific surface area and the presence of H_2O_2 electron capture agent. Firstly, the microflowers have a large surface area due to their entirely hierarchical structure with thin nanoflake building blocks and pores between the sheet layers. This could provide more active catalytic sites for the photocatalytic reactions, allowing maximum absorption and diffuse reflection of sunlight. Secondly, H_2O_2 is a better electron acceptor than molecular oxygen, so it may increase the photocatalyst rate by reducing the chances of electron-hole recombination. When the as-prepared microflowers of CuS are irradiated with sunlight in the presence of H_2O_2, electrons (e^-) and holes (h^+) could be simultaneously excited to the conduction band (CB) and the valence band (VB) edge, and then transferred to the surface of the photocatalyst, where they react with oxidants and reductants respectively, or recombine. In current conditions, these electrons can be captured by H_2O_2 molecules, after which they react with the O_2 in the water to generate a large number of hydroxyl radicals (·OH) and $\cdot O^{2-}$. The h^+ could also react with the water to form ·OH. This could oxidize RhB or MB into intermediates or mineralized products through an oxidation reaction by the so-formed ·OH or $\cdot O^{2-}$. The recombination of e^- and h^+ could be greatly minimized in the presence of H_2O_2. This mechanism is schematically illustrated in Fig. 10.

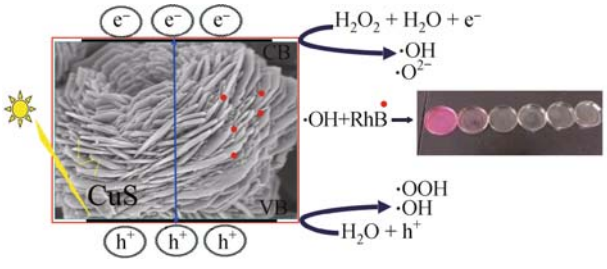

Fig. 10 The schematic diagram illustrating the proposed degradation mechanism of organic pollutants over CuS photocatalyst.

4 Conclusions

In summary, a solvothermal synthesis of CuS hierarchical architectures constructed by nanoflakes is achieved. The results show greatly enhanced visible-light photocatalytic activity for degradation of MB solution. 60% decomposition of RhB dye solution within 5 h is achieved under

natural sunlight irradiation. The extraordinary photocatalytic capability and recycle stability of the hierarchical CuS microflowers with rather high surface area are attributed to the micro scale and the fact that their active components include nano-sized building blocks. This work provides a good way to produce highly efficient photocatalysts, which is of fundamental importance to investigations of their potential use in the development of a hybrid composite with promising applications in water purification.

Acknowledgements We are grateful for the financial support from the National Natural Science Foundation of China (Grant No. 51202156).

References

[1] Armor J N. A history of industrial catalysis. Catalysis Today, 2011, 163(1): 3–9

[2] Kim S D, Cho J, Kim I S, et al. Occurrence and removal of pharmaceuticals and endocrine disruptors in South Korean surface, drinking, and waste waters. Water Research, 2007, 41 (5): 1013–1021

[3] Zhang N, Yang M Q, Tang Z R, et al. Toward improving the graphene-semiconductor composite photoactivity via the addition of metal ions as generic interfacial mediator. ACS Nano, 2014, 8 (1): 623–633

[4] Guo W, Zhang F, Lin C, et al. Direct growth of TiO_2 nanosheet arrays on carbon fibers for highly efficient photocatalytic degradation of methyl orange. Advanced Materials, 2012, 24 (35): 4761–4764

[5] Fan Z, Zhang X, Yang J, et al. Synthesis of 4H/fcc-Au@metal sulfide core–shell nanoribbons. Journal of the American Chemical Society, 2015, 137(34): 10910–10913

[6] Gao W W, Liu W X, Leng Y H, et al. In_2S_3 nanomaterial as a broadband spectrum photocatalyst to display significant activity. Applied Catalysis B: Environmental, 2015, 176–177: 83–90

[7] Xu X J, Hu L F, Gao N, et al. Controlled growth from ZnS nanoparticles to ZnS–CdS nanoparticle hybrids with enhanced photoactivity. Advanced Functional Materials, 2015, 25(3): 445–454

[8] Han S C, Hu L F, Gao N, et al. Efficient self-assembly synthesis of uniform CdS spherical nanoparticles-Au nanoparticles hybrids with enhanced photoactivity. Advanced Functional Materials, 2014, 24(24): 3725–3733

[9] Wang X, Maeda K, Thomas A, et al. A metal-free polymeric photocatalyst for hydrogen production from water under visible light. Nature Materials, 2009, 8(1): 76–80

[10] Zheng Y, Lin L, Ye X, et al. Helical graphitic carbon nitrides with photocatalytic and optical activities. Angewandte Chemie International Edition, 2014, 53(44): 11926–11930

[11] Han C C, Wu L N, Ge L, et al. AuPd bimetallic nanoparticles decorated raphitic carbon nitride for highly efficient reduction of water to H_2 under visible light irradiation. Carbon, 2015, 92: 31–40

[12] Li Y, Shen W. Morphology-dependent nanocatalysts: rod-shaped oxides. Chemical Society Reviews, 2014, 43(5): 1543–1574

[13] Zhang J, Bang J H, Tang C, et al. Tailored TiO_2–$SrTiO_3$ heterostructure nanotube arrays for improved photoelectrochemical performance. ACS Nano, 2010, 4(1): 387–395

[14] Liu S, Tang Z R, Sun Y, et al. One-dimension-based spatially ordered architectures for solar energy conversion. Chemical Society Reviews, 2015, 44(15): 5053–5075

[15] Liu R P, Ren F, Yang J L, et al. One-step synthesis of hierarchically porous hybrid TiO_2 hollow spheres with high photocatalytic activity. Frontiers of Materials Science, 2016, 10 (1): 15–22

[16] Zheng L, Han S, Liu H, et al. Hierarchical MoS_2 nanosheet@TiO_2 nanotube array composites with enhanced photocatalytic and photocurrent performances. Small, 2016, 12(11): 1527–1536

[17] Wang X, Zhuang J, Peng Q, et al. A general strategy for nanocrystal synthesis. Nature, 2005, 437(7055): 121–124

[18] Li X, He X, Shi C, et al. Synthesis of one-dimensional copper sulfide nanorods as high-performance anode in lithium ion batteries. ChemSusChem, 2014, 7(12): 3328–3333

[19] Zhang J, Yu J, Zhang Y, et al. Visible light photocatalytic H_2-production activity of CuS/ZnS porous nanosheets based on photoinduced interfacial charge transfer. Nano Letters, 2011, 11 (11): 4774–4779

[20] Han Y, Wang Y P, Gao W H, et al. Synthesis of novel CuS with hierarchical structures and its application in lithium-ion batteries. Powder Technology, 2011, 212(1): 64–68

[21] Goel S, Chen F, Cai W. Synthesis and biomedical applications of copper sulfide nanoparticles: from sensors to theranostics. Small, 2014, 10(4): 631–645

[22] Cheng Z G, Wang S Z, Wang Q, et al. A facile solution chemical route to self-assembly of CuS ball-flowers and their application as an efficient photocatalyst. CrystEngComm, 2010, 12(1): 144–149

[23] Xu H L, Wang W Z, Zhu W. Sonochemical synthesis of crystalline CuS nanoplates via an *in situ* template route. Materials Letters, 2006, 60(17–18): 2203–2206

[24] Du W, Qian X, Ma X, et al. Shape-controlled synthesis and self-assembly of hexagonal covellite (CuS) nanoplatelets. Chemistry - A European Journal, 2007, 13(11): 3241–3247

[25] Shu Q W, Lan J, Gao M X, et al. Controlled synthesis of CuS caved superstructures and their application to the catalysis of organic dye degradation in the absence of light. CrystEngComm, 2015, 17(6): 1374–1380

[26] Kumar V V, Hariharan P S, Eniyavan D, et al. Alanine based coordinating ligand mediated hydrothermal synthesis of CuS nano/microstructures and morphology dependent photocatalysis. CrystEngComm, 2015, 17(18): 3452–3459

[27] Tanveer M, Cao C B, Aslam I, et al. Synthesis of CuS flowers exhibiting versatile photo-catalyst response. New Journal of Chemistry, 2015, 39(2): 1459–1468

[28] Zhang Y Q, Zhang B P, Ge Z H, et al. Preparation by solvothermal synthesis, growth mechanism, and photocatalytic performance of CuS nanopowders. European Journal of Inorganic Chemistry, 2014, 2014(14): 2368–2375

[29] Mi L, Wei W, Zheng Z, et al. Tunable properties induced by ion exchange in multilayer intertwined CuS microflowers with hierarchal structures. Nanoscale, 2013, 5(14): 6589–6598

[30] Saranya M, Ramachandran R, Samuel E J J, et al. Enhanced visible light photocatalytic reduction of organic pollutant and electrochemical properties of CuS catalyst. Powder Technology, 2015, 279: 209–220

[31] Hosseinpour Z, Alemi A, Khandar A A, et al. A controlled solvothermal synthesis of CuS hierarchical structures and their natural-light-induced photocatalytic properties. New Journal of Chemistry, 2015, 39(7): 5470–5476

[32] Li F, Wu J, Qin Q, et al. Controllable synthesis, optical and photocatalytic properties of CuS nanomaterials with hierarchical structures. Powder Technology, 2010, 198(2): 267–274

[33] Yang Z K, Song L X, Teng Y, et al. Ethylenediamine-modulated synthesis of highly monodisperse copper sulfide microflowers with excellent photocatalytic performance. Journal of Materials Chemistry A: Materials for Energy and Sustainability, 2014, 2 (47): 20004–20009